

tions. Images of neurons were acquired with a charge-coupled device camera with a 60× oil-immersion objective (numerical aperture = 1.4) affixed to an inverted microscope and quantitated with Metamorph imaging software. For each neuron studied, the three largest caliber proximal dendrites (~20 μm long) were analyzed. To quantitate changes in clustering, we measured the average pixel intensities of all synaptic clusters along these dendritic segments in transfected and neighboring nontransfected cells and analyzed data by paired *t* test. All clusters that colocalized with synaptophysin and were at least twice the background intensity were analyzed.

11. S. E. Craven, A. E. Husseini, D. S. Bredt, *Neuron* **22**, 497 (1999).
12. D. B. Arnold, D. E. Clapham, *Neuron* **23**, 149 (1999).
13. Supplementary figures are available at *Science* Online at www.sciencemag.org/cgi/content/full/290/5495/1364/DC1.
14. Whole-cell recordings were made at room temperature from 11- to 13-day-old cultured neurons, with 4- to 6-megohm patch pipettes. Pipette solutions contained (in mM) 94 Cs-glucuronate, 2 CsCl, 8 tetraethylammonium-Cl, 4 QX-314Cl, 7 NaCl, 8 Hepes, 0.2 EGTA, 3 MgATP, 0.3 Na₂GTP, and 0.02 to 0.1% Lucifer yellow CH. Cultures were continuously superfused with buffer containing (in mM) 112 NaCl, 3 KCl, 16 glucose, 8 Hepes, 2 CaCl₂, 2 MgCl₂, 0.1 picrotoxin, and 0.001 tetrodotoxin at 1 ml/min. Cells were patched under visual guidance with a water-immersion microscope. Transfected cells were identified before recording by fluorescence. Current records were low-pass filtered at 2 kHz, stored on tape, and digitized off-line at 5 kHz. Cells were held at -70 mV, and recording stability was monitored in real time with -4-mV steps every 10 s. Series resistances ranged between 15 and 25 megohm. Recordings were made for 2 to 10 min from each cell, depending on mEPSC frequency (cells with higher frequencies were recorded for less time). mEPSCs were analyzed with customized software (E. Schnell), with an amplitude threshold of 5 pA. To control for variability, neighboring transfected and untransfected cells were selected for recording. Transfected and untransfected cells were compared with the unpaired *t* test. To assess spine morphology, 21 or 22 DIV neurons were filled with 0.1% Lucifer yellow for 3 min, fixed in paraformaldehyde, and stained for GAD-65 to exclude interneurons. Images were taken with a 100× oil-immersion objective, and an observer blinded with respect to neuronal transfection quantitated spine size and density.
15. Although increases in mEPSC frequency typically reflect increased probability of transmitter release, an enlarged mEPSC amplitude can also increase apparent frequency, because very small events can be amplified to the detection threshold. To determine whether a change in mEPSC detection might account for the increase in frequency, we made additional recordings from cultured neurons at different holding potentials to manipulate mEPSC amplitude. In these experiments, an increase of mEPSC amplitude that corresponded to the observed difference between untransfected and PSD-95-transfected pyramidal cells (from 8.4 ± 0.3 pA to 11.4 ± 0.2 pA, *n* = 4) was associated with a 2.9 ± 0.6-fold increase in the mEPSC frequency. Because the transfected neurons had a 9.8 ± 2.9-fold greater mEPSC frequency, the change in mEPSC detection is unable to account for the increase in frequency, confirming that a change in presynaptic function has occurred.
16. A. J. Cochilla, J. K. Angleson, W. J. Betz, *Annu. Rev. Neurosci.* **22**, 1 (1999).
17. E. Kim *et al.*, *J. Cell Biol.* **136**, 669 (1997).
18. S. Naisbitt *et al.*, *Neuron* **23**, 569 (1999).
19. Z. Nusser *et al.*, *Neuron* **21**, 545 (1998).
20. R. S. Petralia *et al.*, *Nature Neurosci.* **2**, 31 (1999).
21. S. N. Gomperts, R. Carroll, R. C. Malenka, R. A. Nicoll, *J. Neurosci.* **20**, 229 (2000).
22. R. A. McKinney, M. Capogna, R. Dürr, B. H. Gähwiler, S. M. Thompson, *Nature Neurosci.* **2**, 44 (1999).
23. A. S. Leonard, M. A. Davare, M. C. Horne, C. C. Garner, J. W. Hell, *J. Biol. Chem.* **273**, 19518 (1998).
24. An increase in mEPSC frequency can result from an increase in the probability of transmitter release from

an individual synapse and/or from an increase in the number of synapses. It has been reported that the probability of release is related to the size of the vesicle pool (33). Given the lack of change in the number of synapses contacting PSD-95-transfected cells in DIV 12 neurons (untransfected: GluR1 puncta = 0.614 ± 0.054 μm⁻²; PSD-95-GFP: GluR1 puncta = 0.714 ± 0.054 μm⁻²; *P* > 0.05), we conclude that much of the change is due to an increase in release probability secondary to the larger vesicle pool implied by the enhanced synaptophysin and FM4-46 staining.

25. M. Gautam *et al.*, *Nature* **377**, 232 (1995).
26. M. Irie *et al.*, *Science* **277**, 1511 (1997).
27. K. Ichtchenko *et al.*, *Cell* **81**, 435 (1995).
28. P. Scheiffele, J. Fan, J. Chioh, R. Fetter, T. Serafini, *Cell* **101**, 657 (2000).
29. M. Maletic-Savatic, R. Malinow, K. Svoboda, *Science* **283**, 1923 (1999).

30. A. W. McGee, D. S. Bredt, *J. Biol. Chem.* **274**, 17431 (1999).
31. H. Shin, Y. P. Hsueh, F. C. Yang, E. Kim, M. Sheng, *J. Neurosci.* **20**, 3580 (2000).
32. J. E. Brenman, K. S. Christopherson, S. E. Craven, A. W. McGee, D. S. Bredt, *J. Neurosci.* **16**, 7407 (1996).
33. V. N. Murthy, T. J. Sejnowski, C. F. Stevens, *Neuron* **18**, 599 (1997).
34. We thank R. Edwards, M. von Zastrow, and G. Davis for critical reviews of earlier versions of the manuscript. Supported by grants from the NIH (R.A.N. and D.S.B.), Howard Hughes Medical Institute Research Resources Program (D.S.B.), and Human Frontier Research Program (D.S.B.). D.M.C. is a postdoctoral fellow of the Howard Hughes Medical Institute, A.E.-D.E.-H. is supported by a grant from the Medical Research Council of Canada and E.S. is supported by the Medical Scientist Training Program.

19 July 2000; accepted 20 October 2000

Intracellular Parasitism by *Histoplasma capsulatum*: Fungal Virulence and Calcium Dependence

Tricia Schurtz Sebghati, Jacquelyn T. Engle, William E. Goldman*

Histoplasma capsulatum is an effective intracellular parasite of macrophages and causes the most prevalent fungal respiratory disease in the United States. A "dimorphic" fungus, *H. capsulatum* exists as a saprophytic mold in soil and converts to the parasitic yeast form after inhalation. Only the yeasts secrete a calcium-binding protein (CBP) and can grow in calcium-limiting conditions. To probe the relation between calcium limitation and intracellular parasitism, we designed a strategy to disrupt *CBP1* in *H. capsulatum* using a telomeric linear plasmid and a two-step genetic selection. The resulting *cbp1* yeasts no longer grew when deprived of calcium, and they were also unable to destroy macrophages *in vitro* or proliferate in a mouse model of pulmonary infection.

Histoplasma capsulatum is a pathogenic fungus that is a major cause of respiratory and systemic mycosis, especially in immunocompromised individuals (1). Histoplasmosis occurs worldwide but is endemic in the Mississippi and Ohio River valleys in the United States, where the organism thrives in soil in its mycelial (mold) form. As with most other dimorphic fungal pathogens, conversion to a unicellular haploid yeast form occurs after inhalation and exposure to the warmer temperature of the respiratory tract (2). There, *H. capsulatum* is readily engulfed by macrophages, in which the yeasts survive and proliferate within the normally hostile environment of phagolysosomes (3). The characteristics of this particular intracellular compartment are poorly understood, although we have previously demonstrated that *Histoplasma*-laden phagolysosomes fail to acidify (4).

Studies with *Salmonella typhimurium*, which also survives within phagolysosomes of macrophages, have suggested that this compartment is low in Ca²⁺ concentration (5).

The latter observation may have particular relevance for *H. capsulatum*, as we have observed a major difference in calcium dependence between the saprophytic (mycelial) form and the parasitic (yeast) form. *Histoplasma capsulatum* yeasts are capable of growing in a calcium-deprived environment and secrete a 7.8-kD calcium-binding protein (CBP); in contrast, mycelial cultures do not secrete CBP and require calcium for growth (6). The CBP structural gene, *CBP1*, has been cloned and sequenced, and a potential calcium binding site is predicted from the secondary structure of CBP (7). Purified CBP has also been shown to increase the association of ⁴⁵CaCl₂ with *H. capsulatum* yeasts after they have been transferred to low-calcium medium (7). To verify the functional role of CBP in calcium acquisition and/or virulence, we devised a generally applicable gene-disruption strategy for *Histoplasma*: Linear telomeric plasmids and a two-step gene-

Department of Molecular Microbiology, Campus Box 8230, Washington University School of Medicine, St. Louis, MO 63110, USA.

*To whom correspondence should be addressed. E-mail: goldman@borcim.wustl.edu

REPORTS

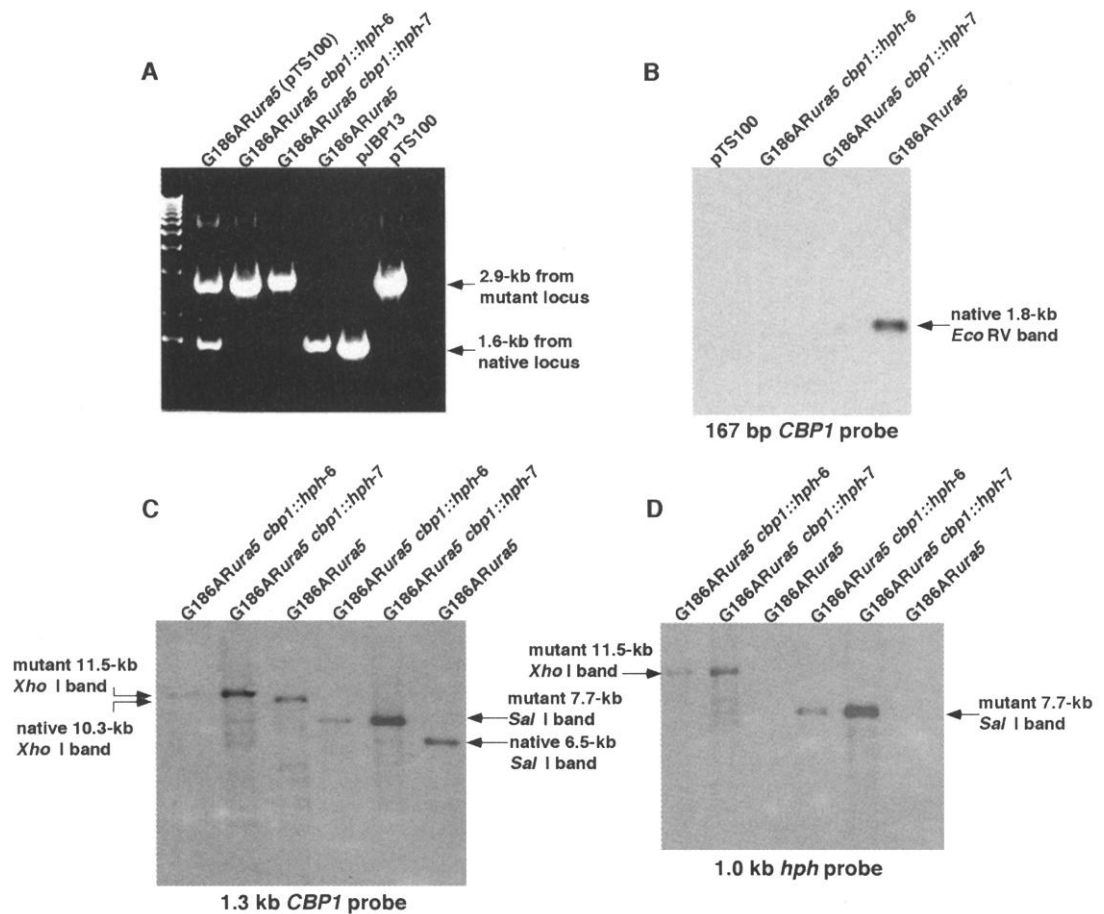
netic selection were used to inactivate the *CBP1* gene by allelic replacement. This work showed that CBP is critical for virulence and for calcium uptake by *H. capsulatum* yeasts, suggesting that this intracellular parasite has evolved a means to cope effectively with a calcium-limiting environment in vivo.

For most pathogenic fungi, classical recombinational analysis is either impossible or extremely tedious (8). Transformation of *H. capsulatum* with plasmid DNA usually results in random integration of the DNA into the genome, often accompanied by tandem amplification and rearrangement of the transforming DNA (9, 10). Illegitimate recombination events so greatly outnumber homologous recombination events that it is impractical to detect the desired gene disruption; to date, only the counterselectable *URA5* gene has been successfully knocked out in *H. capsulatum* (11). To prevent the high frequency of nonhomologous recombination, we designed a two-step gene-disruption strategy

that uses a linearized telomeric vector maintained extrachromosomally in high copy number (10, 12, 13). This telomeric plasmid (pTS100) contains two selectable markers, a *URA5* gene located on an arm of the vector and a hygromycin-resistance cassette (*hph*) located within the *CBP1* gene (replacing a portion of the coding sequence) [Web fig. 1 (14)] (13, 15). In the first selection step, this construct was used to transform a uracil auxotroph (16, 17) of a virulent strain of *H. capsulatum* (18). G186ARura5 (pTS100) transformants were initially grown on HMM agar (19) lacking uracil to select for yeasts that were maintaining the transformed DNA as a freely replicating linear plasmid. Six colony-purified yeast isolates were then inoculated into HMM broth without uracil and maintained for 3 weeks with regular medium changes. This length of time allows the desired double-crossover event to occur; the use of a linear plasmid vector ensures that single crossovers into the genome would break the

chromosome and presumably be lethal. In the second step of this strategy, a positive-negative selection was applied with hygromycin and 5-fluoro-orotic acid (5-FOA), which inhibits the growth of uracil prototrophs. This step enriches for recombinants at the *CBP1* locus by simultaneously selecting for stable maintenance of the disrupted gene (containing the hygromycin-resistance cassette) and selecting against the *URA5*-containing plasmid vector. Each of the six broth cultures was plated on solid medium containing hygromycin and 5-FOA, and an isolated colony from each culture was grown in broth under the same selection conditions for three additional weeks. Total genomic DNA was prepared from six colony-purified putative mutants and used as a template for polymerase chain reaction (PCR) and Southern analysis (20, 21). The results indicate that an allelic replacement of *CBP1* with *cbp1::hph* had occurred in two out of six of the putative mutants (Fig. 1). This knockout strategy was

Fig. 1. (A) PCR was performed with genomic DNA isolated from pTS100 transformants and from transformation recipient strain G186ARura5. Oligonucleotide primers were targeted to the 5' and 3' regions of *CBP1*: The forward primer spanned bases 100 to 117 of *CBP1* and the reverse primer spanned bases 1727 to 1747 of the *CBP1* gene. A transformant in which homologous recombination had not occurred [G186ARura5 (pTS100)] showed a PCR product that resulted from retention of the telomeric plasmid (2.9 kb) and its native chromosomal *CBP1* locus (1.6 kb). Hygromycin- and 5-FOA-resistant transformants G186ARura5 *cbp1::hph-6* and *-7* have undergone an allelic replacement in *CBP1* and therefore showed a single PCR product (2.9 kb). The recipient strain G186ARura5 showed only an intact *CBP1* PCR product (1.6 kb). The predicted 1.6-kb *CBP1* product was also amplified from wild-type *CBP1* on plasmid pJBP13, and a 2.9-kb *cbp1::hph* product was amplified from disruption plasmid pTS100. For Southern analysis, restriction digests of genomic DNAs from transformants, as well as the transformation recipient strain G186ARura5, were subjected to electrophoresis, blotted, and hybridized with three probes: a 167-base pair (bp) fragment spanning the *Sma*I-*Msc*I deletion that was replaced by the *hph* cassette (B), a 1.3-kb fragment spanning bases 1 to 1313 from *CBP1* (C), and a 1.0-kb fragment spanning bases 1 to 1023 of the *hph* cassette (D). Hybridization of the *CBP1* probe to DNA from transformants G186ARura5 *cbp1::hph-6* and *-7* did not detect the native genomic *CBP1* but instead detected an 11.5-kb



Xho I band or a 7.7-kb Sal I band (C). This same probe detected bands corresponding to native *CBP1* (a 10.3-kb Xho I fragment or a 6.5-kb Sal I fragment) in recipient strain G186ARura5 DNA (C), which did not hybridize to an *hph* gene probe (D). DNA from transformants 6 and 7 also did not hybridize to a 167-bp probe spanning the *Sma*I/*Msc*I *CBP1* deletion, whereas DNA from recipient strain G186ARura5 hybridized to this probe (B).

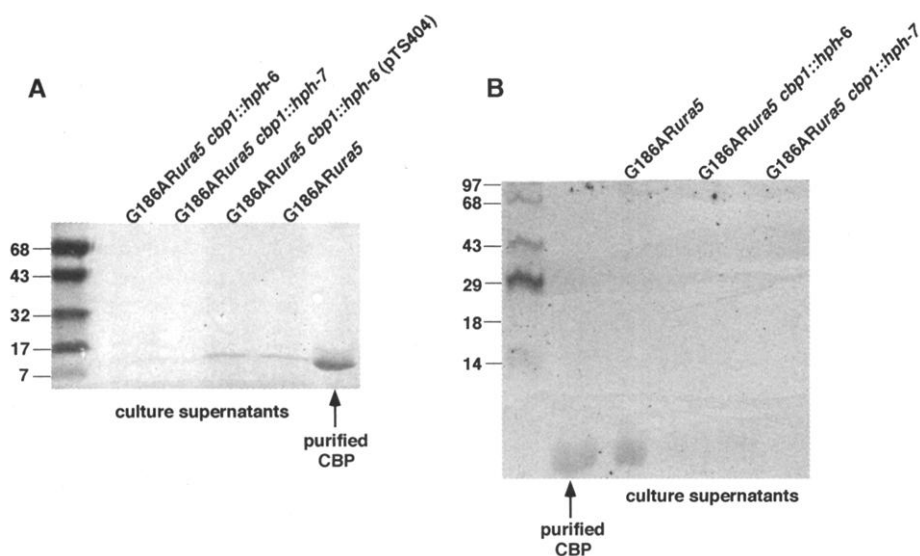


Fig. 2. (A) Ruthenium red staining of purified CBP or culture supernatant from *H. capsulatum* after SDS-PAGE and transfer to nitrocellulose. (B) $^{45}\text{CaCl}_2$ blot of purified CBP or culture supernatant after SDS-PAGE and transfer to nitrocellulose.

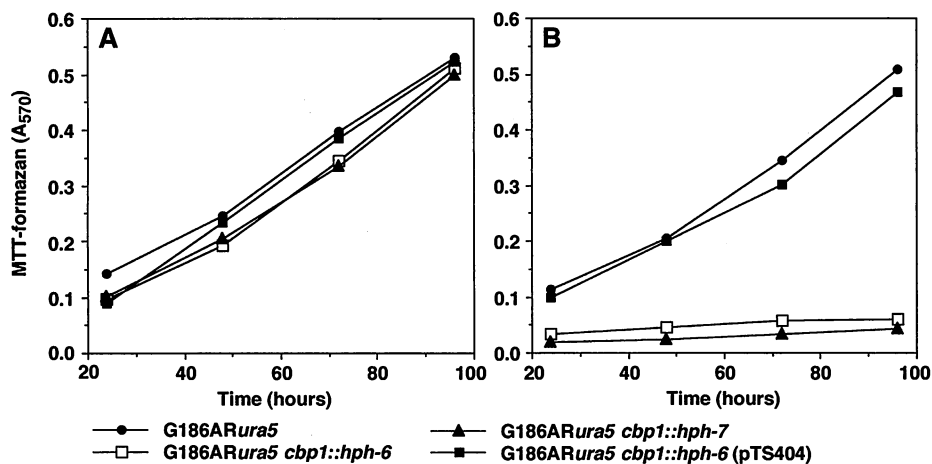


Fig. 3. *Histoplasma capsulatum* *cbp1::hph* yeasts were grown in HMM medium in the presence or absence of EGTA. Metabolic activity as measured by MTT assays was used to monitor culture health and growth over time. (A) G186ARura5 *cbp1::hph-6*, -7, and G186ARura5 *cbp1::hph-6* (pTS404) exhibited growth rates similar to that of parental strain G186ARura5 in standard growth medium HMM (supplemented with uracil as needed). (B) In the presence of 150 μM EGTA, growth of strains G186ARura5 *cbp1::hph-6* and -7 was inhibited. The CBP1-complemented strain, G186ARura5 *cbp1::hph-6* (pTS404), grew as well as parental strain G186ARura5 in the presence of EGTA.

repeated in the same strain (G186ARura5) and in a genetically unrelated strain, G217Bura5, with the same plasmid construct. In both cases (and despite some sequence heterogeneity with *CBP1* in strain G217Bura5), a similar frequency of allelic replacement with *cbp1::hph* was confirmed, indicating that this strategy is an efficient and reproducible method for gene disruption in *H. capsulatum*.

To demonstrate that CBP from *H. capsulatum* *cbp1::hph* isolates was no longer able to bind calcium, we prepared $^{45}\text{CaCl}_2$ blots (22). Purified CBP and CBP in culture supernatants from parental strain G186ARura5 bound $^{45}\text{CaCl}_2$, but proteins in culture supernatants

from *H. capsulatum* G186ARura5 *cbp1::hph-6* and -7 did not bind (Fig. 2). These results were confirmed by Ruthenium red staining for calcium-binding proteins (22, 23): Although CBP could be detected in strain G186ARura5 culture supernatant, filtrates from *cbp1::hph* isolates had no detectable CBP (Fig. 2). Growth of *cbp1*-knockout yeasts in medium deprived of calcium was measured metabolically over time by monitoring reduction of 3-[4,5 dimethylthiazol-2-yl]-2,5-diphenyltetrazolium bromide (MTT) (24, 25). The parent strain G186ARura5 grew well under all conditions tested; however, isolates disrupted in *CBP1* were unable to grow in calcium-limited medium (Fig. 3).

To confirm that the phenotypes associated with the *cbp1*-knockouts are the result of the targeted mutation, we constructed an isogenic strain that contains *CBP1* in trans. The plasmid, pTS404, was designed in the same manner as pTS100 [Web fig. 1 (14)], including 5'- and 3'-untranslated regions flanking the intact *CBP1* gene. The complementation plasmid also included the *Podospora URA5* gene and contained telomeric repeats for stable maintenance in *Histoplasma*. This plasmid was introduced by electrotransformation, and its extrachromosomal replication was subsequently confirmed by Southern blot analysis (26). The complemented strain G186ARura5 *cbp1::hph-6* (pTS404) regained the ability to secrete CBP in quantities comparable to that secreted by wild-type yeasts (Fig. 2). Introduction of *CBP1* in trans also restored this knockout strain's ability to grow in media deprived of calcium by EGTA (Fig. 3).

Because *H. capsulatum* yeasts are normally capable of proliferating in and destroying macrophages, we have developed a quantitative in vitro macrophage model for virulence that uses P388D1.D2 cells (a macrophage-like cell line) (3, 27). This assay is based on the relative ability of a defined number of yeasts to kill macrophages in a given period of time (27). Strain-specific differences in the ability to kill P388D1.D2 cells correlate with virulence as measured in standard animal models of histoplasmosis. In its current version, this in vitro assay measures the amount of macrophage DNA remaining in a monolayer after infection by *H. capsulatum* yeasts (28), using an ultrasensitive fluorescent stain specific for double-stranded DNA. The *cbp1*-knockout strain was unable to destroy P388D1.D2 cells after 7 to 10 days of infection, whereas the parental strain G186ARura5 did. Complementation of this *cbp1*-knockout strain with *CBP1* in trans restored virulence to a level similar to that of the parent strain (Fig. 4A). Phenotypic complementation was not achieved with pTS105 (26), which is an identical plasmid construct except for a short deletion within the *CBP1* coding sequence [Web fig. 1 (14)].

Because CBP proved to be vital for *Histoplasma* pathogenesis in macrophages, we evaluated the virulence of a *cbp1*-null strain of *H. capsulatum* in a murine model of respiratory infection (29). Mice, like many other mammals, are natural hosts for *H. capsulatum*, and the progression of pathology, dissemination, and immunity closely parallels human histoplasmosis (30). For animal infections, mice were inoculated intranasally with the *H. capsulatum* strains indicated in Fig. 4B. After 8 days, the lungs were removed to count the number of viable *H. capsulatum* yeasts. The number of G186ARura5 (pWU55) yeasts recovered from the lungs was more than 10-fold higher than the number administered intranasally 8 days earlier.

REPORTS

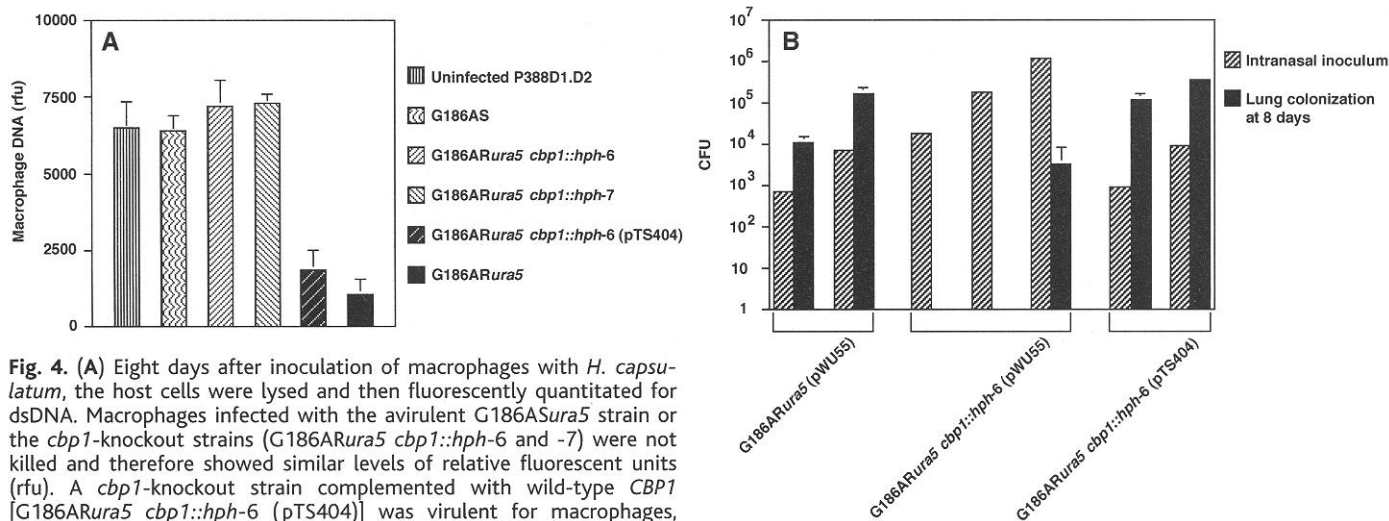


Fig. 4. (A) Eight days after inoculation of macrophages with *H. capsulatum*, the host cells were lysed and then fluorescently quantitated for dsDNA. Macrophages infected with the avirulent G186ASura5 strain or the *cbp1*-knockout strains (G186ARura5 *cbp1::hph-6* and *-7*) were not killed and therefore showed similar levels of relative fluorescent units (rfu). A *cbp1*-knockout strain complemented with wild-type *CBP1* [G186ARura5 *cbp1::hph-6* (pTS404)] was virulent for macrophages, yielding results comparable to those for infection with the G186ARura5 parental strain. Data shown are representative of three experiments and are expressed as the mean \pm SE. **(B)** In this mouse model of pulmonary colonization, relative virulence of each strain can be evaluated by comparing the mean colony-forming units (CFU) inoculated intranasally and later recovered from mice at 8 days after infection.

Data are representative of two experiments and are expressed as the mean \pm SE per lung. The telomeric plasmid pWU55, which contains *URA5*, was transformed into strains G186ARura5 and G186ARura5 *cbp1::hph-6* to restore uracil prototrophy, which is required for virulence in vivo (32).

er. Disrupting *CBP1* in G186ARura5 rendered these yeasts unrecoverable from lung tissue, except when the infecting dose was increased more than 1000-fold; even then, the number of yeasts recovered from the lung was greatly reduced from the original intranasal inoculum. These results do not reflect a simple growth defect in the *cbp1*-null strain, because all strains tested in mice have a similar generation time when grown in broth culture (26). When the *cbp1*-knockout strain was complemented by addition of *CBP1* in trans, pulmonary colonization by the yeasts was restored to a level comparable to that of the virulent G186ARura5 (pWU55) strain.

In summary, *CBP* was indispensable for the virulence of *H. capsulatum* yeasts in vitro and in vivo, as well as for the growth of *H. capsulatum* in limiting calcium conditions. How *CBP* links both of these phenotypes remains unknown, but the simplest hypothesis is that calcium acquisition is an important strategy for microbial survival in this intracellular compartment. Alternatively, *CBP* may bind calcium in order to modulate phagolysosomal conditions that might otherwise inhibit yeast survival. For example, chelation of calcium could restrict the destructive power of some lysosomal enzymes, and a recent report shows that limiting calcium during formation of endosomes inhibits their normal acidification (31). This correlates with the failure of phagosomes containing *Histoplasma* to acidify (4), potentially pointing to a mechanism of avoiding intracellular destruction by lysosomal enzymes that typically have a low pK.

This study also presents a formal genetic proof of a virulence determinant in *H. capsulatum*. This gene-targeting strategy should

be generally applicable to probing gene function in *H. capsulatum* and other closely related dimorphic fungal pathogens, which have similar problems in genetic manipulation that pose formidable barriers in testing the roles of putative virulence factors.

References and Notes

1. J. R. Graybill, *J. Infect. Dis.* **158**, 623 (1988); R. P. Baughman *et al.*, *Am. Rev. Respir. Dis.* **134**, 771 (1986).
2. L. G. Eissenberg, W. E. Goldman, *Clin. Microbiol. Rev.* **4**, 411 (1991); J. W. Rippon, in *Medical Mycology, The Pathogenic Fungi and the Pathogenic Actinomycetes*, M. L. W. R. Wonsiewicz, Ed. (Saunders, Philadelphia, PA, 1988), p. 381; R. A. Goodwin, J. L. Shapiro, G. H. Thurman, S. S. Thurman, R. M. Des Perez, *Medicine* **59**, 1 (1980).
3. L. G. Eissenberg, P. H. Schlesinger, W. E. Goldman, *J. Leukocyte Biol.* **43**, 483 (1988).
4. L. G. Eissenberg, W. E. Goldman, P. H. Schlesinger, *J. Exp. Med.* **177**, 1605 (1993).
5. E. García Vescovi, Y. M. Ayala, E. Di Cera, E. Groisman, *J. Biol. Chem.* **272**, 1440 (1997).
6. J. W. Batanghari, W. E. Goldman, *Infect. Immun.* **65**, 5257 (1997); S. Kügler, B. Young, V. L. Miller, W. E. Goldman, *Cell. Microbiol.* **2**, 549 (2000).
7. J. W. Batanghari, G. S. Deepe Jr., E. Di Cera, W. E. Goldman, *Mol. Microbiol.* **27**, 531 (1998).
8. L. H. Hogan, B. S. Klein, *Gene* **186**, 219 (1997); A. Varma, J. C. Edman, K. J. Kwon-Chung, *Infect. Immun.* **60**, 1101 (1992).
9. P. L. Worsham, W. E. Goldman, *Mol. Gen. Genet.* **214**, 348 (1988).
10. J. P. Woods, W. E. Goldman, *Mol. Microbiol.* **6**, 3603 (1992).
11. J. P. Woods, D. M. Retallack, E. L. Heinecke, W. E. Goldman, *Infect. Immun.* **180**, 5135 (1998).
12. J. P. Woods, W. E. Goldman, *J. Bacteriol.* **175**, 636 (1993).
13. J. P. Woods, E. L. Heinecke, W. E. Goldman, *Infect. Immun.* **66**, 1697 (1998).
14. Supplementary data are available at Science Online at www.sciencemag.org/cgi/content/full/290/5495/1368/DC1.
15. P. J. Punt, R. P. Oliver, M. A. Dingemans, P. H. Pouwels, C. A. M. J. van den Hondel, *Gene* **56**, 117 (1987).
16. Ultraviolet (UV) light mutagenesis was performed on late exponential phase yeast cells (4×10^8 /ml)

grown in HMM medium (19), placed on ice for 20 min, and centrifuged (110g, 60 s) to remove large aggregates. The yeast suspension was diluted with fresh, ice-cold HMM to a density of 10^7 colony-forming units (CFU) per milliliter. An ultraviolet (UV) germicidal lamp was used at a distance of 64 cm to irradiate the yeasts. Yeast cells were stirred during the 40-s exposure to UV light. The cells were washed with ice-cold HMM and plated on selective medium containing 5-FOA (1 mg/ml) and uracil (100 μ g/ml). All manipulations after exposure to UV light were performed in the dark to prevent photoreactivation repair. Plates were incubated at 37°C with 95% air, 5% CO₂ in a humidified incubator. Colonies arising on HMM with 5-FOA-uracil were picked 3 weeks after plating and streaked for isolation on the same medium. Single colonies were picked and replated onto HMM with and without uracil. Several independent isolates exhibited uracil auxotrophy in the yeast phase, and one of these isolates also exhibited auxotrophy when grown as mycelia at room temperature.

17. Before its introduction into yeasts, each plasmid (2 μ g) was linearized by digestion with Pac I. The linear telomeric plasmid was purified by gel electrophoresis to separate it from the kanamycin-resistance cassette, and the plasmid was concentrated by ethanol precipitation. The plasmid DNA was introduced into yeasts by electroporation (13). Briefly, 5 ml of a 2-day culture was centrifuged at 300g for 5 min. The supernatant was discarded and the yeasts were resuspended in 5 ml of warm (37°C), 10% (w/v) mannitol. The yeasts were recovered by centrifugation, as above, and resuspended in 200 μ l of 10% (w/v) mannitol. The yeasts were mixed with the plasmid DNA in a 0.2-cm cuvette at room temperature. The electroporations were done at a capacitance of 25 μ F, a resistance of 600 ohm, and a voltage of 0.75 kV. Time constants were between 10 and 12 ms. The electroporated cells were directly plated onto HMM without uracil and incubated at 37°C for 12 to 14 days.
18. The virulent strain used in this study, *H. capsulatum* G186AR, has been described previously (27). Unless otherwise indicated, *H. capsulatum* was grown as described for yeast cells at 37°C in the defined medium HMM (19). In some experiments, uracil (100 μ g/ml), hygromycin B (100 μ g/ml), and/or 5-FOA (1 mg/ml) were added to solid or liquid HMM.
19. P. L. Worsham, W. E. Goldman, *J. Med. Vet. Mycol.* **26**, 137 (1988).
20. Total genomic DNA from *Histoplasma* was purified as

REPORTS

- previously described (10). Southern blotting and PCR were done according to standard procedures (21). DNA probes were labeled and signals were detected with enhanced chemiluminescence direct nucleic acid labeling and detection systems (Amersham Life Science, Arlington Heights, IL).
21. J. Sambrook, E. F. Fritsch, T. Maniatis, *Molecular Cloning: A Laboratory Manual* (Cold Spring Harbor Laboratory Press, Cold Spring Harbor, NY, ed. 2, 1998); F. M. Ausubel et al., Eds., *Current Protocols in Molecular Biology* (Wiley, New York, 2000).
 22. For $^{45}\text{CaCl}_2$ blotting, proteins in concentrated culture supernatants were separated by SDS-polyacrylamide gel electrophoresis (PAGE) and transferred to 0.1- μm nitrocellulose. After incubation in calcium-free hybridization buffer [10 mM tris-HCl (pH 6.8), 60 mM KCl, and 5 mM MgCl_2], the filter was probed with $^{45}\text{CaCl}_2$ (3 $\mu\text{Ci/ml}$) for 8 hours at 37°C, followed by washing for 5 min with water at pH 6.8. The filter was exposed for autoradiography. Ruthenium red staining was performed by blotting proteins as described above, then incubating the nitrocellulose in Ruthenium red (25 mg/liter).
 23. J. H. M. Charuk, C. A. Pirraglia, R. A. F. Reithmeier, *Anal. Biochem.* **188**, 123 (1990).
 24. S. M. Levitz, R. D. Diamond, *J. Infect. Dis.* **152**, 938 (1985).
 25. For growth of yeast in calcium-limiting conditions, *H. capsulatum* strains G186ARura5 and G186ARura5 *cbp1::hph-6* and *-7* were inoculated at 1×10^6 yeast cells/ml into 24-well plates in HMM supplemented with 150, 300, or 600 μM EGTA to chelate the 300 μM Ca^{2+} present in HMM. Growth was monitored spectrophotometrically at an optical density of 600 nm. Metabolic activity was measured by the reduction of MTT to purple crystals of formazan and quantitated by measuring the absorbance at 570 nm.
 26. T. Schurtz Sebhathi, J. T. Engle, W. E. Goldman, data not shown.
 27. L. G. Eissenberg, J. L. West, J. P. Woods, W. E. Goldman, *Infect. Immun.* **59**, 1639 (1991).
 28. The in vitro virulence assay uses P388D1.D2 cells, a randomly selected clone from P388D1 macrophage-like cells (27), which were seeded at a 2×10^4 cells per 7-mm well in F-12 completed with 10% fetal bovine serum. The monolayers were inoculated in triplicate with dispersed yeasts in HMM-M completed with 10% fetal bovine serum (3), supplemented with uracil for auxotrophs, with a yeast:host cell ratio of 1:5. The 96-well microtiter plates were rocked continuously on a rocking platform to facilitate coculture of these cells. The medium was replaced with fresh medium at 3 days after inoculation and every other day thereafter. Using phase-contrast microscopy, we examined the wells daily to estimate when ~95% of the macrophage monolayer was destroyed by wild-type virulent yeasts. At this time (8 days), all medium was removed, and wells were washed three times with sterile phosphate-buffered saline to remove any lysed cells or free yeast cells. The macrophages were then lysed by addition of sterile distilled water (pH 7.0), which does not lyse yeast cells. The fluorescent PicoGreen double-stranded DNA (dsDNA) quantitation reagent (Molecular Probes, Sunnyvale, CA) was used to measure the amount of macrophage DNA present in each well. The fluorescence intensity was measured with a FluorImager SI (Molecular Probes) at 530 nm.
 29. Male Balb/C57BL/6J mice were purchased from Jackson Laboratories. Mice were infected intranasally with *H. capsulatum* cells in a 50- μl volume. For all strains tested, we inoculated three animals with each inoculum dose. After 8 days, the animals were killed and the lungs were homogenized in HMM medium and serially diluted and dispensed (50 μl) into HMM pour agar plates supplemented with 10 μM FeSO_4 . Plates were incubated at 37°C, and CFU were counted after 10 days. To determine actual intranasal inoculum, yeasts were appropriately diluted and plated, and CFU were counted.
 30. G. S. Deepe, W. E. Bullock, *Eur. J. Clin. Microbiol. Infect. Dis.* **9**, 567 (1990).
 31. J. V. Gerasimenko, A. V. Tepikin, O. H. Petersen, O. V. Gerasimenko, *Curr. Biol.* **8**, 1335 (1998).
 32. D. M. Retallack, E. L. Heinecke, R. Gibbons, G. S. Deepe Jr., J. P. Woods, *Infect. Immun.* **67**, 624 (1999).
 33. We thank J. West Batanghari and J. Balduz Patel for preliminary experiments on *CBP1* disruption in *H. capsulatum*. Supported by Public Health Service grants AI25584 (to W.E.G.) and A107172 and HL07317 (to Washington University). W.E.G. is a recipient of the Burroughs Wellcome Fund Scholar Award in Molecular Pathogenic Mycology.

30 June 2000; accepted 19 September 2000

Science ~~ONLINE~~

Take a hike!

In our Enhanced Perspectives, we navigate the virtual forest for you. Each week, one Perspective from *Science's Compass* links readers to the best related Web-based content:

- research databases
- tutorials
- glossaries
- abstracts
- other online material

Take your virtual hike at www.sciencemag.org/misc/e-perspectives.shtml